PHILOSOPHICAL TRANSACTIONS B

Phil. Trans. R. Soc. B.
doi:10.1098/rstb.2015.0510

Biogeochemical significance of Pelagic Ecosystem Function: An end-Cretaceous Case Study

Michael J. Henehan[1]*, Pincelli M. Hull[1], Donald E. Penman[1], James W. B. Rae[2] and Daniela N. Schmidt[3]

[1] Department of Geology and Geophysics, Yale University, 210 Whitney Avenue, New Haven, CT-06511 USA. ORCID (MH): 0000-0003-4706-1233
[2] Department of Earth Sciences, Irvine Building, University of St. Andrews, St. Andrews KY16 9AL, UK ORCID: 0000-0001-8419-2721
[3] Department of Earth Sciences, University of Bristol, Wills Memorial Building, Queens Road, Bristol BS8 1RJ, UK.

Keywords: biogeochemical cycling, ecosystem function, Cretaceous-Palaeogene extinction, bolide impact, LOSCAR, mass extinction

Main Text

Summary

Pelagic ecosystem function is integral to global biogeochemical cycling, and plays a major role in modulating atmospheric CO_2 concentrations (pCO_2). Uncertainty as to the effects of human activities on marine ecosystem function hinders projection of future atmospheric pCO_2. To this end, events in the geological past can provide informative case studies in the response of ecosystem function to environmental and ecological changes. Around Cretaceous-Palaeogene (K-Pg) boundary, two such events occurred: Deccan large igneous province (LIP) eruptions and massive bolide impact at the Yucatan Peninsula. Both perturbed the environment, but only the impact coincided with marine mass extinction. As such, we use these events to directly contrast the response of marine biogeochemical cycling to environmental perturbation with and without changes in global species richness. We measure this biogeochemical response using records of deep-sea carbonate preservation. We find that Late Cretaceous Deccan volcanism prompted transient deep-sea carbonate dissolution, of a larger magnitude and timescale than predicted by geochemical models. Even so, the effect of volcanism on carbonate preservation was slight compared to bolide impact. Empirical records and geochemical models support pronounced increase in carbonate saturation state for •500,000 years following the mass extinction of pelagic carbonate producers at the K-Pg boundary. These examples highlight the importance of pelagic ecosystems in moderating climate and ocean chemistry.

Introduction

Atmospheric CO_2 concentrations (pCO_2) are regulated by a complex, interconnected system of sources and sinks, both abiotic and biotic [e.g. 1,2,3]. Biological activity in the surface oceans plays a major role in this via the "biological carbon pump", whereby pelagic organisms take up carbon in the surface ocean, die and sink, sequestering carbon in the deep ocean. In addition, pelagic calcifying organisms (such as coccolithophores and planktonic foraminifera) export $CaCO_3$ to the deep oceans, sequestering weathering products from land in sediments (the "alkalinity pump"). This balances alkalinity fluxes, provides a dissolvable carbonate reservoir that buffers the ocean from potentially-harmful pH change, and helps to maintain largely equable climates [4,5]. Together, planktonic foraminifera and coccolithophores account for the vast majority of the pelagic carbonate flux[6], which in turn accounts for almost half of total marine carbonate production[7]. As such, pelagic organisms play an important role in biogeochemical cycling and climate regulation.

Human activities (examples among many include injection of CO_2, overfishing, oxygen depletion, and

*Author for correspondence (Michael.Henehan@yale.edu).
†Present address: Department of Geology and Geophysics, Yale University, 210 Whitney Avenue, New Haven CT-06511, USA.

habitat destruction) threaten the function of the pelagic ecosystem [8–10], adding uncertainty to the projection of pCO_2 and climate over the coming centuries [3,11]. In part, this uncertainty stems from a lack of available ecological datasets across the spatial and temporal scales that would be relevant in constraining model predictions [12]. Most existing ecological time series are too short to discern trends beyond decadal variation in the climate system and relatively few studies have addressed the link between biodiversity and ecosystem function on geological time scales (see [13] in this issue for an exception). The microfossil record can be a useful resource in addressing these knowledge gaps [14], and placing constraints on the response of the pelagic ecosystem to environmental perturbations and their effect on biogeochemical cycles. During a ~ 1 million year (Myr) interval surrounding the Cretaceous-Palaeogene (K-Pg) boundary 66.04 Myr ago, two very different disturbances are recorded in the marine fossil record. These events provide case studies on the interplay between environmental change, biodiversity and ecosystem function under similar background conditions. Our study thereby begins to address a gap in our current understanding of the relationship between biodiversity and ecosystem function [13,15].

The onset of vast flood basalt volcanism (the Deccan Large Igneous Province LIP) in the latest Cretaceous resulted in the release of 15,000 – 35,000 Gt CO_2 and 6,400 - 17,000 Gt SO_2, over a relatively long (>100,000 yr) timescale [16,17]. In contrast, the impact of a ~10 km-wide bolide at Chicxulub at the K-Pg boundary [18] led to instantaneous release of SO_x, NO_x and CO_2 [19 and references within] and rapid and transient (probably <5yr) acidification of the surface ocean [20,21]. Besides the very different timescales of these environmental perturbations, a critical difference is that the Chicxulub impact coincides with a major mass extinction and Late Cretaceous Deccan volcanism does not [19]. Species loss in the open ocean following the bolide impact, while variable between groups [22], was particularly high in the calcareous plankton (~95 and 90% in planktonic foraminifera and calcareous nannofossils respectively[23,24]). In contrast, during Late Cretaceous Deccan trap volcanism, biotic disturbance in the open ocean was largely limited to changes in biogeographic ranges [e.g. 25,26]. Together, these events allow us to contrast the impact of environmental changes on ecosystem function with and without associated loss of pelagic biodiversity. Here we use carbonate preservation indices to gain a fuller understanding of changes in biogeochemical ecosystem function across this interval, combining new and previously published records of carbonate preservation from geographically disparate deep-sea sites with new insights from ocean carbon cycle modelling.

Methods: Carbonate Preservation

Change in deep ocean carbonate saturation state ($\bullet_{CaCO3}$) is an indicator of broader carbon cycle disturbance that can be readily discerned in the geological record using records of deep-sea carbonate preservation [e.g. 27]. New and previously published records of a number of different $CaCO_3$ preservational indices are compiled here from globally-distributed deep-sea drill core sediments over a 3.7 million year (myr) interval surrounding the K-Pg boundary, 66.04 million years ago. Each $CaCO_3$ preservation metric has associated strengths and limitations, which we discuss at length in the Supplementary Information. Where possible, our new records of deep sea preservation use counts of planktonic foraminiferal fragmentation [as in 28,29]. This metric relies on the observation that with decreasing deep ocean $\bullet_{CaCO3}$ microfossils progressively dissolve and fragment [30] (see Fig. S1). New fragmentation data were generated from Shatsky Rise in the Pacific (Ocean Drilling Program (ODP) Site 1209) and Walvis Ridge in the South Atlantic (ODP Site 1267). Meaningful fragmentation counts from Newfoundland Sediment Drifts site in the North Atlantic (International Ocean Drilling Program (IODP) Site U1403) were not attainable due to extensive dissolution prior to the K-Pg boundary (see Fig. S2). At this site, weight per cent (wt. %) coarse fraction (>38 µm) was used as a carbonate preservation indicator (though important caveats to this production-sensitive metric are discussed in the supplement). Sediment samples were dried and weighed, before being disaggregated in de-ionised water on an orbital shaker and washed through a 63 µm (Walvis Ridge, Site 1267 & Shatsky Rise, Site 1209) or 38 µm (Newfoundland, Site U1403) sieve with de-ionised water. Both the >63 µm />38 µm coarse fraction and the fine fraction were then dried at ~45°C and the coarse fraction weighed to calculate wt. % coarse fraction. For Walvis Ridge (Site 1267) and Shatsky Rise (Site 1209), the relative abundance of 'complete' tests (i.e. whole tests that show no signs of any breakage or dissolution of chambers) was counted from a representative split (200 - 400 fossils) of the >125 µm size fraction. Full details of the methods used to construct age models for each site (including the construction of new age models for previously published data) are given in the Supplementary Information.

Methods: Carbon cycle modelling

The geochemical box model LOSCAR (Long-term Ocean Sediment Carbon Reservoir) version 2.0.4 [31] was employed to simulate the impacts of volcanic degassing and calcifier extinction on the global carbon cycle, with some modifications. Importantly, to better account for the very different [Ca^{2+}] and [Mg^{2+}] in the K-Pg ocean [32], updated carbonate chemical equilibrium constants from the MyAMI model [33] were substituted into the model, using a [Ca^{2+}] of 42 mmol/kg and [Mg^{2+}] of 20 mmol/kg. All plotted model runs (Figs. 3, S5-11) were initiated at a steady state pCO_2 of 600 ppm (in agreement with palaeosol carbonate measurements [34,35, and references therein]), and assume a climate sensitivity of 3 °C per doubling of pCO_2. This climate sensitivity is in the middle of the range (2.2 – 4.8 ˚C) of observed climate sensitivity over the past 65 Ma [36]. However, a range of other starting atmospheric CO_2 concentrations (400-1000 ppm) and climate sensitivities (0-5 ˚C per doubling) were also explored, with results listed in Table S1 (see also Supplementary Discussion). Our primary experiments (Fig. 3) also assume a stronger-than-modern silicate weathering feedback, to account for a greater abundance of exposed fresh Deccan basalt at low latitudes (see Supplementary Information for more details), although model runs at a range of feedback strengths were also tested (see Table S1, Figure S10).

For simulations of Deccan degassing, minimum and maximum emission scenarios (total CO_2 = 4,090 or 9,500 Gt C, total SO_2 = 3,200 or 8,500 Gt S [16]) were partitioned into two discrete pulses, in accordance with the proposed second and third stages of volcanism from [37], and the eruptive volumes of [38]. 86.5% of degassing was input over a ~140kyr interval beginning at the C30n/C29r magnetochron reversal, approximately 360 kyr before the K-Pg boundary. This corresponds to an observed interval of decreasing seawater $^{187}Os/^{188}Os$ (which indicates elevated basalt weathering) [39]. The remaining 13.5% of the volcanic emissions was then released in models at the end of magnetochron C29r in the Danian (250 kyr after the K-Pg boundary). Most other estimates of CO_2 release for the Deccan Traps [38,40–42] fall within the range of emissions tested here [16]. To better discern the effects of each gas, scenarios for CO_2 and SO_2 release were also tested in isolation (Fig. 3). As in [21], SO_2 release and rain-out were simulated by reducing alkalinity in the surface ocean box (see Supplement for more details). A wide range of possible timescales and modes of degassing were also tested (see Supplementary Information, Table S1).

For simulations of the biogeochemical consequences of the K-Pg mass extinction, a range of carbonate flux reductions were tested, ranging from 10% up to 75%. We tested two types of scenarios: i) reductions in $CaCO_3$ flux with no change in the organic carbon flux (i.e., a change in the C_{CaCO3}:C_{org} flux ratio), and ii) reductions in overall efficiency of the biological carbon and alkalinity pump (i.e., reducing both C_{CaCO3} and C_{org} fluxes). For each simulation, changes in fluxes were imposed for 200 kyr following the K-Pg boundary and then tapered back to pre-event values over a further 200 kyr to simulate the gradual recovery of early Palaeocene pelagic ecosystems. For further details and discussion about modelling approaches, see Supplementary Information.

Deccan Volcanism, Global Warming & Carbonate Dissolution

The main phase of Deccan volcanism [37] is recorded in deep-sea sediments by a global decline in $^{187}Os/^{188}Os$ [39] just after the C30n/C29r magnetochron reversal [17] at 66.398 Ma (Figure 1a). The onset of volcanism and associated release of CO_2 coincides with evidence for a transient warming event (see Fig. 1b) in both geochemical [44–47] and palaeoecological data [e.g. 25,48,49]. Our data show a pronounced increase in deep-sea carbonate dissolution in several ocean basins at this time, in response to this volcanism (Figure 1c-h). Dissolution is particularly pronounced in the Southern Ocean (ODP Site 690 [39,50,51], Fig. 1c) and North Atlantic (IODP Site U1403 [52], Fig. 1d) , with weight per cent (wt. %) carbonate falling by ~20 % and~40 %, respectively. This result is consistent with enhanced dissolution in high-latitude sediments closest to sites of deep water formation [53], where the impact of increased CO_2 emissions will first be felt. At lower latitudes, increased foraminiferal fragmentation is seen at Walvis Ridge (ODP Site 1267, Fig. 1e [this study]; DSDP Site 527, Fig. 1f [54]) and Shatsky Rise (ODP Site 1209, Fig. 1g [this study]), are indicative of a shoaling of the lysocline (i.e. the depth at which substantial carbonate dissolution occurs). Reduced planktonic foraminiferal preservation elsewhere on Shatsky Rise (DSDP Site 577 [55]; Fig. 1h), and selective preservation of dissolution-resistant coccolithophores in the Indian Ocean [50] (Fig. S4) corroborate this observation.

In all cases, records of increased dissolution return to roughly pre-event values before the K-Pg boundary (Fig. 1), restricting the main degassing phase of Deccan Volcanism to a distinct <200 kyr interval beginning at the onset of magnetochron C29r, around 66.398 Ma. This supports previous inferences for only transient ocean acidification based on Ir accumulation [39], and suggests Deccan degassing played no direct role in K-Pg mass extinction. New absolute age constraints for the Deccan eruptions [17] have been cited as evidence of a Deccan role in the K-Pg extinction through ocean acidification [56]. Our data (and modelling below and Figs. S5, S6) suggest that even these new timescales for eruption are still long enough for surface ocean carbonate saturation to be maintained via carbonate compensation and silicate weathering [see also 57].

Bolide Impact and Mass Extinction at the K-Pg

In the aftermath of the K-Pg, sediment records from the Pacific and Atlantic (Fig. 2) show a pronounced rise in wt. % coarse fraction, as a result of both decreased calcareous plankton production and enhanced foraminiferal preservation. Simultaneously, fragmentation of planktonic foraminifera at both Walvis Ridge [43] and Shatsky Rise [28] declines (Fig. 2), even to essentially no fragmentation at Shatsky Rise. Since some foraminiferal fragmentation is normally expected during sinking and sedimentation even above the lysocline [58,59] (see Fig. S1), this lack of discernible fragmentation at Shatsky Rise indicates very high [CO_3^{2-}] throughout the water column. Rapid and pronounced deepening of the lysocline due to this enhanced [CO_3^{2-}] is evidenced at the Newfoundland Sediment Drift in the North Atlantic (IODP Site U1403), where we observed a step-change across the K-Pg from Maastrichtian sediments barren of any planktonic foraminifera to post-boundary sediments in which Danian planktonic foraminiferal species are excellently preserved (Fig. S2) up until around magnetochron C28r (see Fig 2). Similarly, in the South Pacific (IODP Site U1370, 5076m depth) [60] the only carbonate preserved over the last 75 Myr is in the immediate aftermath of the K-Pg boundary, within nannofossil zones NP1 and NP2[60]. Elsewhere, at the Ontong-Java plateau (ODP Site 803, 3410m depth), carbonate is preserved for a brief interval (<1m, within biozone NP1) around the K-Pg boundary, but is absent above and below[61]. Additional lines of evidence for a rise in oceanic $\bullet_{CaCO3}$, are also discussed in the supplement (Section 6d). These lines of sedimentological evidence all support the predictions of earlier work [62,63] that reduced pelagic carbonate production due to extinction of calcareous plankton following the K-Pg bolide impact [64,65] profoundly impaired the marine alkalinity pump (a key pelagic ecosystem function) and prompted a period of alkalinity build-up, deepening of the lysocline, and ocean pH rise.

Comparison with Carbonate System Models

Using the LOSCAR carbon-cycle model [31], we attempt to reproduce observed patterns of environmental change and deep-sea carbonate preservation. For pre-boundary volcanism, we find that only high-end Deccan CO_2 emission scenarios can produce the widely observed late Maastrichtian warming of ~2-3 °C at mid-range climate sensitivity (3 °C/CO_2 doubling), for an initial atmospheric pCO_2 of 600ppm [34] and an eruptive duration of 140kyr. Moreover, with this forcing only high-strength silicate weathering feedbacks (see Supplementary Discussion) could draw down CO_2 and temperature within only several hundred thousand years, consistent with observations (Fig 1b). For lower CO_2 emission scenarios, either high-end late Cretaceous climate sensitivity (>3 °C/CO_2 doubling) or lower initial pCO_2 are required to produce observed warming (see Table S1).

In terms of carbonate cycle perturbation, LOSCAR predicts at most only fleeting reductions (< 40 kyr) in either surface or deep ocean $\bullet_{CaCO3}$ for an eruptive duration of 140 kyr (Fig. 3, Fig. S5), although a ~0.5 Myr reduction in surface ocean pH of up to 0.19 is predicted (Fig S5). For even the largest estimates of SO_2 and CO_2 release, LOSCAR suggests that eruptive timescales of < 100 kyr are required to produce pronounced lysocline shoaling (Fig. S6), and even then this shoaling would be briefer (<50 kyr) than indicated in the sedimentary record (~150-200 kyr, Fig. 1 c-h). Instead, the dominant long-term signal predicted for Deccan CO_2 release under any modelled emissions scenario is elevated weathering fluxes, a rise in oceanic carbonate saturation, and a deepening of the lysocline (Fig. 3). We observe little evidence for this enhanced preservation (or 'carbonate overshoot') following the initial dissolution pulse of Deccan volcanism (Fig. 1c-h). The brevity of dissolution relative to preservation records and the existence of a pronounced carbonate overshoot are consistent in all modelled scenarios, despite different timescales for release, total emissions, starting pCO_2, equilibrium constants and weathering feedbacks (see Supplementary Discussion and Table S1).

There are multiple possible explanations for this mismatch between empirical observations and model predictions (discussed in depth in the Supplementary Information), including an overestimation of the duration of the Cretaceous portion of magnetochron C29r [as suggested by recent U-Pb dating; 17], changes in circulation or productivity, elevated $CaCO_3$ deposition in shelf settings (see Fig S9) or the influence of processes not accounted for in LOSCAR. Another possible explanation is that Deccan-induced warming resulted in a more stratified ocean with more oligotrophic surface waters [e.g. 49,48,26]. In the modern ocean, oligotrophy favours ecosystems more heavily dominated by coccolithophore production as compared to siliceous and organic-walled primary producers[e.g. 66]. If this was similar in the Cretaceous ocean, and Deccan warming did indeed result in enhanced stratification and more oligotrophic oceans, it is possible that $CaCO_3$ production and export rose. A modelled increase in $CaCO_3$:C_{org} ratio of 30% during simulated warming succeeds in extending the timescales of deep-ocean carbonate dissolution to approximate agreement with sedimentary records, amplifying atmospheric CO_2 rise, and dampening subsequent carbonate saturation increase (Fig. S8). This emphasises the potential importance of accounting for biotic, ecological feedbacks when considering the ocean's response to greenhouse gas forcings.

We also simulate the effects of an extinction of pelagic carbonate producers at the K-Pg boundary (Fig. 3, S5, S11). Although the bolide impact [20,21], and a brief reduction in photosynthetic carbon uptake [43] could have induced acidification of surface waters and released CO_2 from the oceans on timescales of <10 kyr [63] (Fig. 3), the more significant long-term impact on the carbon cycle comes about from the major extinction in both main groups of pelagic calcifiers. This extinction, and loss of abundance, caused changes in carbonate saturation state that persisted for > 1 Myr (Fig. 2). We demonstrate that even a conservative 30% reduction of $CaCO_3$ export flux results in a deepening of the Atlantic carbonate compensation depth (CCD) by 2 km, an increase in surface • from 6.6 to 10 (Fig. S11) and a drop in atmospheric CO_2 of ~100 ppm (Fig. 3), consistent with modelled findings of earlier studies [62,63]. This elevation of ocean alkalinity in response to mass extinction could provide a mechanism for low atmospheric pCO_2 estimated for the early Danian [67]. Our modelling suggests a 30% drop in $CaCO_3$ export would also lower the modelled Pacific CCD to ~4200 m: enough to bring the CCD below the South Pacific Gyre IODP Site U1370 but remain above Site U1365, consistent with sedimentary observations [60]. Deep-sea sediment cores, though, suggest a much greater reduction in pelagic $CaCO_3$ production and delivery [43 and references within]. In our model runs, a reduction in $CaCO_3$ production by > 50 % would produce sufficiently high supersaturation to initiate abiotic precipitation of $CaCO_3$ in surface waters (Fig. S10); a process which today is not known beyond tropical shelf settings such as the Bahamas or Persian Gulf. While there is perhaps some evidence for this [68], it is also possible that other synchronous changes may have occurred to avoid critical supersaturation. Increased burial of carbonate on shelves to compensate for less deep-ocean burial could have played a role [63] (see also Fig. S9), although evidence for such an increase is, at best, scant (see Supplementary Discussion).

Volcanism, Impact, & the Carbon Cycle: Implications for Biodiversity and Ecosystem Function

Environmental forcing imposed by Deccan emplacement and K-Pg bolide impact produced very different recorded changes in ecosystem function (Figs 1-2), primarily as a result of very different patterns of ecological response. There is little evidence for loss of species or population abundance in the open ocean plankton during Late Cretaceous Deccan volcanism. The ~2-3 °C warming associated with Deccan CO_2 release resulted in range expansions [25,26,48], dwarfing of some planktonic foraminiferal species [69], and regional assemblage changes [70], but there was no elevation in extinction rates of functionally important marine calcifier species (planktonic foraminifera and coccolithophores) at this time [65,71]. This retention of biodiversity and redundancy among calcifiers, we suggest, was likely important in maintaining the resilience of the pelagic ecosystem (and its associated biogeochemical functions) [15,72]. Consequently the marine carbonate cycle, coupled with global silicate weathering feedbacks [1], could assimilate Deccan-derived CO_2 over these timescales without drastic, long-lasting effects on surface ocean $\bullet_{CaCO3}$ (only very modest lysocline shallowing and some reduction in surface ocean pH, see Fig S5, are indicated). This role of pelagic calcifiers in mitigating the impact of CO_2 emissions is underscored by considering similar volcanic episodes before the evolution of pelagic calcifiers [4,5]. Two of these earlier episodes, the end-Triassic Central Atlantic Magmatic Province [73] and Permo-Triassic Siberian Traps [74] volcanism, had profound environmental impacts and resulted in two of the largest mass extinctions in the history of life [5].

The more profound and long-lasting perturbation of surface ocean carbonate saturation we observe over the K-Pg transition arises from mass extinction following the Chicxulub bolide impact. The near-complete loss of the clades responsible for the vast majority of pelagic carbonate cycling (planktonic foraminifera and coccolithophores [64,65]) resulted in a build up of alkalinity in the Earth's ocean (as evidenced by improved deep-ocean carbonate preservation; Fig. 2). This in turn may have also drawn down atmospheric CO_2 and prompted climatic changes [62, this study]. While some evidence suggests export of organic carbon to the deep ocean had largely recovered within a few hundred thousand years [75,76], carbonate preservation (Fig. 2) suggests recovery of full pre-event biogeochemical function in pelagic ecosystems took more than a million years, coinciding with restoration of micro- and nannofossil biodiversity [e.g. 77]: an example of the close link between biosphere and geosphere dynamics in the aftermath of mass extinction [see also 78].

Current global change is altering pelagic ecosystems, but the extent of this alteration in biodiversity [9] and ecosystem structure [79] and its ultimate biogeochemical significance, remains unclear [2,3]. In the case of the K-Pg boundary, the extinction was particularly selective against pelagic calcifiers, and post-extinction ecosystems lacked both the diversity and abundance of pre-extinction oceans. Although it is the decline in calcifier abundance that directly accounts for the decline in ecosystem function, it remains an open question how important standing richness is, within and across calcifier clades, in determining calcifier abundance across the event. It is noteworthy in this context that post-extinction biogeochemical function (and by inference the abundance of calcifiers) recovers long in advance of the full recovery of pre-event levels of calcifier diversity (see Fig. 2; also [80]). This observation suggests that while functional redundancy among latest Cretaceous calcareous plankton may have helped to confer resilience on carbonate export [72] in the face of volcanic CO_2 and SO_x emissions and global warming, a much lower standing diversity can still support a comparable carbonate alkalinity pump. For the oceans today, it is crucial to determine where tipping points may lie with regards to shifting the abundance of marine organisms, as it is the aggregate effect of many, many billions that account for pelagic ecosystem function. As we show here, pelagic ecosystem change, particularly in pelagic calcifiers, can profoundly influence on the long-term evolution of the Earth system.

Additional Information

Acknowledgments
We thank Richard Zeebe for provision of, and assistance with, LOSCAR, and Leanne Elder for laboratory assistance. This work contains data and imaging contributions from Alex Twiney, Megan Mikenas and Liana Epstein. Greg Ravizza, Ellen Thomas, Jens and Ines Wendler, Mathis Hain, Michal Kucera and Björn Malmgren are thanked for helpful discussion, as well as Gavin Foster for his contributions during the early development of the project. We thank the IODP for provision of sample material. We thank Moriaki Yasuhara and other anonymous reviewers for their constructive comments.

Data Accessibility
The datasets supporting this article have been uploaded as part of the Supplementary Material (Tables S2 and S3), and will in due course be made available via www.Pangaea.de.

Authors' Contributions
MJH collected data, constructed age models, steered modelling and drafted the manuscript and figures. PMH directed the study, and assisted in drafting the manuscript. DEP carried out carbon cycling modelling and assisted in drafting the manuscript. JWBR co-supervised data collection and assisted in drafting the manuscript. DNS directed the early stages of this project and assisted in drafting the manuscript.

Competing Interests
We have no competing interests.

Funding
This work was aided by a Nuffield Summer Studentship granted to MJH, a U.S. Science Support Program (USSSP) Post-Expedition Activity award for IODP Exp. 342 to PMH, a Flint Postdoctoral Fellowship to DEP, a NERC PhD Studentship granted to JWBR, and a URF and Wolfson merit award to DNS.

References

1. Berner, R. A., Lasaga, A. C. & Garrels, R. M. 1983 The carbonate-silicate geochemical cycle and its effect on atmospheric carbon dioxide over the past 100 million years. *Am. J. Sci.* **283**, 641–683. (doi:10.2475/ajs.283.7.641)
2. Gruber, N., Friedlingstein, P., Field, C. B., Valentini, R., Heimann, M., Richey, J. E., Lankao, P. R., Schulze, E. D. & Chen, C.-T. A. 2004 The Vulnerability of the carbon cycle in the 21st century: An assessment of carbon-

climate-human interactions. In *The Global Carbon Cycle: Integrating Humans, Climate and the Natural World* (eds C. B. Field & M. R. Raupach), pp. 45–76. Washington D. C.: Island Press.

3. Ciais, P. et al. 2013 Carbon and Other Biogeochemical Cycles. In *Climate Change 2013: The Physical Science Basis. Contribution of Working Group I to the Fifth Assessment Report of the Intergovernmental Panel on Climate Change* (eds T. F. Stocker & et al.), pp. 465–570. Cambridge: Cambridge University Press.

4. Zeebe, R. E. & Westbroek, P. 2003 A simple model for the $CaCO_3$ saturation state of the ocean: The 'Strangelove,' the 'Neritan,' and the 'Cretan' Ocean: MODEL FOR $CACO_3$ SATURATION STATE. *Geochem. Geophys. Geosystems* **4**, n/a–n/a. (doi:10.1029/2003GC000538)

5. Ridgwell, A. J. & Zeebe, R. E. 2005 The role of the global carbonate cycle in the regulation and evolution of the Earth system. *Earth Planet. Sci. Lett.* **234**, 299–315. (doi:10.1016/j.epsl.2005.03.006)

6. Schiebel, R. 2002 Planktic foraminiferal sedimentation and the marine calcite budget. *Glob. Biogeochem. Cycles* **16**, 1065. (doi:10.1029/2001GB001459)

7. Milliman, J. D. 1993 Production and accumulation of calcium carbonate in the ocean: Budget of a nonsteady state. *Glob. Biogeochem. Cycles* **7**, 927–957. (doi:10.1029/93GB02524)

8. Tyrrell, T. 2011 Anthropogenic modification of the oceans. *Philos. Trans. R. Soc. Lond. Math. Phys. Eng. Sci.* **369**, 887–908. (doi:10.1098/rsta.2010.0334)

9. Pörtner, H.-O., Karl, D., Boyd, P. W., Cheung, W., Lluch-Cota, S. E., Nojiri, Y., Schmidt, D. N. & Zavialov, P. 2014 Ocean Systems. In *Climate Change 2014: Impacts, Adaptation, and Vulnerability. Part A: Global and Sectoral Aspects. Contribution of Working Group II to the Fifth Assessment Report of the Intergovernmental Panel on Climate Change* (eds C. B. Field V. R. Barros D. J. Dokken K. J. Mach M. D. Mastrandrea T. E. Bilir M. Chatterjee K. L. Ebi R. C. Estrada R. C. Genova et al.), pp. 411–484. Cambridge, UK and New York, USA: Cambridge University Press.

10. Worm, B. et al. 2006 Impacts of Biodiversity Loss on Ocean Ecosystem Services. *Science* **314**, 787–790. (doi:10.1126/science.1132294)

11. Mora, C. et al. 2013 Biotic and Human Vulnerability to Projected Changes in Ocean Biogeochemistry over the 21st Century. *PLoS Biol.* **11**, e1001682. (doi:10.1371/journal.pbio.1001682)

12. Henson, S. A., Sarmiento, J. L., Dunne, J. P., Bopp, L., Lima, I., Doney, S. C., John, J. & Beaulieu, C. 2010 Detection of anthropogenic climate change in satellite records of ocean chlorophyll and productivity. *Biogeosciences* **7**, 621–640. (doi:10.5194/bg-7-621-2010)

13. Yasuhara, M., Doi, H., Wei, C.-L., Danovaro, R. & Myhre, S. E. 2016 Biodiversity-ecosystem functioning relationships in long-term time series and palaeoecological records: deep sea as a test bed. *Philosphical Trans. R. Soc. B* **this issue**.

14. Yasuhara, M., Tittensor, D. P., Hillebrand, H. & Worm, B. 2015 Combining marine macroecology and palaeoecology in understanding biodiversity: microfossils as a model: Marine macroecology-palaeoecology integration. *Biol. Rev.* , n/a–n/a. (doi:10.1111/brv.12223)

15. Brose, Ü. & Hillebrand, H. 2016 Biodiversity and ecosystem functioning in dynamic landscapes. *Philos. Trans. R. Soc. B*

16. Chenet, A.-L., Courtillot, V., Fluteau, F., Gérard, M., Quidelleur, X., Khadri, S. F. R., Subbarao, K. V. & Thordarson, T. 2009 Determination of rapid Deccan eruptions across the Cretaceous-Tertiary boundary using paleomagnetic secular variation: 2. Constraints from analysis of eight new sections and synthesis for a 3500-m-thick composite section. *J. Geophys. Res. Solid Earth* **114**, B06103. (doi:10.1029/2008JB005644)

17. Schoene, B., Samperton, K. M., Eddy, M. P., Keller, G., Adatte, T., Bowring, S. A., Khadri, S. F. R. & Gertsch, B. 2015 U-Pb geochronology of the Deccan Traps and relation to the end-Cretaceous mass extinction. *Science* **347**, 182–184. (doi:10.1126/science.aaa0118)

18. Alvarez, L. W., Alvarez, W., Asaro, F. & Michel, H. V. 1980 Extraterrestrial Cause for the Cretaceous-Tertiary Extinction. *Science* **208**, 1095–1108. (doi:10.1126/science.208.4448.1095)

19. Schulte, P. et al. 2010 The Chicxulub Asteroid Impact and Mass Extinction at the Cretaceous-Paleogene Boundary. *Science* **327**, 1214–

1218. (doi:10.1126/science.1177265)

20. Ohno, S. et al. 2014 Production of sulphate-rich vapour during the Chicxulub impact and implications for ocean acidification. *Nat. Geosci.* **7**, 279–282. (doi:10.1038/ngeo2095)

21. Tyrrell, T., Merico, A. & Armstrong McKay, D. I. 2015 Severity of ocean acidification following the end-Cretaceous asteroid impact. *Proc. Natl. Acad. Sci.* , 201418604. (doi:10.1073/pnas.1418604112)

22. Alegret, L., Thomas, E. & Lohmann, K. C. 2012 End-Cretaceous marine mass extinction not caused by productivity collapse. *Proc. Natl. Acad. Sci.* **109**, 728–732. (doi:10.1073/pnas.1110601109)

23. Gallala, N., Zaghbib-Turki, D., Arenillas, I., Arz, J. A. & Molina, E. 2009 Catastrophic mass extinction and assemblage evolution in planktic foraminifera across the Cretaceous/Paleogene (K/Pg) boundary at Bidart (SW France). *Mar. Micropaleontol.* **72**, 196–209. (doi:10.1016/j.marmicro.2009.05.001)

24. D'Hondt, S., Herbert, T. D., King, J. & Gibson, C. 1996 Planktic foraminifera, asteroids, and marine production: Death and recovery at the Cretaceous-Tertiary boundary. In *Special Paper 307: The Cretaceous-Tertiary Event and Other Catastrophes in Earth History*, pp. 303–317. Geological Society of America. [cited 2015 Jun. 5].

25. Olsson, R. K., Wright, J. D. & Miller, K. G. 2001 Paleobiogeography of Pseudotextularia Elegans During the Latest Maastrichtian Global Warming Event. *J. Foraminifer. Res.* **31**, 275–282. (doi:10.2113/31.3.275)

26. Thibault, N., Gardin, S. & Galbrun, B. 2010 Latitudinal migration of calcareous nannofossil Micula murus in the Maastrichtian: Implications for global climate change. *Geology* **38**, 203–206. (doi:10.1130/G30326.1)

27. Zachos, J. C. et al. 2005 Rapid Acidification of the Ocean During the Paleocene-Eocene Thermal Maximum. *Science* **308**, 1611–1615. (doi:10.1126/science.1109004)

28. Hancock, H. J. L. & Dickens, G. R. 2005 Carbonate Dissolution Episodes in Paleocene and Eocene Sediment, Shatsky Rise, West-Central Pacific. *Proc. Ocean Drill. Program Sci. Results* **Leg 198**.

29. Colosimo, A. B., Bralower, T. J. & Zachos, J. C. 2006 Evidence for lysocline shoaling at the Paleocene/Eocene Thermal Maximum on Shatsky Rise, northwest Pacific. In *Proceedings of the Ocean Drilling Project, Scientific Results* (eds T. J. Bralower I. Premoli Silva & M. J. Malone), pp. 1–36. College Station, TX.

30. Berger, W. H., Bonneau, M.-C. & Parker, F. L. 1982 Foraminifera on the deep-sea floor: lysocline and dissolution rate. *Oceanol. Acta* **5**, 249–258. (doi:0399-1784/1982/249)

31. Zeebe, R. E. 2012 LOSCAR: Long-term Ocean-atmosphere-Sediment CArbon cycle Reservoir Model v2.0.4. *Geosci Model Dev* **5**, 149–166. (doi:10.5194/gmd-5-149-2012)

32. Stanley, S. M. & Hardie, L. A. 1998 Secular oscillations in the carbonate mineralogy of reef-building and sediment-producing organisms driven by tectonically forced shifts in seawater chemistry. *Palaeogeogr. Palaeoclimatol. Palaeoecol.* **144**, 3–19. (doi:10.1016/S0031-0182(98)00109-6)

33. Hain, M. P., Sigman, D. M., Higgins, J. A. & Haug, G. H. 2015 The effects of secular calcium and magnesium concentration changes on the thermodynamics of seawater acid/base chemistry: Implications for Eocene and Cretaceous ocean carbon chemistry and buffering. *Glob. Biogeochem. Cycles* , 2014GB004986. (doi:10.1002/2014GB004986)

34. Nordt, L., Atchley, S. & Dworkin, S. 2003 Terrestrial evidence for two greenhouse events in the latest Cretaceous. *GSA Today* **13**, 4–9.

35. Nordt, L., Atchley, S. & Dworkin, S. I. 2002 Paleosol barometer indicates extreme fluctuations in atmospheric CO2 across the Cretaceous-Tertiary boundary. *Geology* **30**, 703–706. (doi:10.1130/0091-7613(2002)030<0703:PBIEFI>2.0.CO;2)

36. Rohling, E. J. et al. 2012 Making sense of palaeoclimate sensitivity. *Nature* **491**, 683–691. (doi:10.1038/nature11574)

37. Chenet, A.-L., Quidelleur, X., Fluteau, F., Courtillot, V. & Bajpai, S. 2007 40K-40Ar dating of the Main Deccan large igneous province: Further evidence of KTB age and short duration. *Earth Planet. Sci. Lett.* **263**, 1–15.

(doi:10.1016/j.epsl.2007.07.011)

38. Self, S., Widdowson, M., Thordarson, T. & Jay, A. E. 2006 Volatile fluxes during flood basalt eruptions and potential effects on the global environment: A Deccan perspective. *Earth Planet. Sci. Lett.* **248**, 518–532. (doi:10.1016/j.epsl.2006.05.041)

39. Robinson, N., Ravizza, G., Coccioni, R., Peucker-Ehrenbrink, B. & Norris, R. 2009 A high-resolution marine 187Os/188Os record for the late Maastrichtian: Distinguishing the chemical fingerprints of Deccan volcanism and the KP impact event. *Earth Planet. Sci. Lett.* **281**, 159–168. (doi:10.1016/j.epsl.2009.02.019)

40. Jay, A. E. & Widdowson, M. 2008 Stratigraphy, structure and volcanology of the SE Deccan continental flood basalt province: implications for eruptive extent and volumes. *J. Geol. Soc.* **165**, 177–188. (doi:10.1144/0016-76492006-062)

41. Caldeira, K. & Rampino, M. R. 1990 Carbon dioxide emissions from Deccan volcanism and a K/T boundary greenhouse effect. *Geophys. Res. Lett.* **17**, 1299–1302.

42. McLean, D. M. 1985 Deccan Traps Mantle Degassing in the Terminal Cretaceous Marine Extinctions. *Cretac. Res.* **6**, 235–259.

43. D'Hondt, S. 2005 Consequences of the Cretaceous/Paleogene Mass Extinction for Marine Ecosystems. *Annu. Rev. Ecol. Evol. Syst.* **36**, 295–317. (doi:10.1146/annurev.ecolsys.35.021103.105715)

44. Stott, L. D. & Kennett, J. P. 1990 The paleoceanographic and paleoclimatic signature of the Cretaceous/Paleogene boundary in the Antarctic: stable isotopic results from ODP Leg 113. In *Proceedings of the Ocean Drilling Project*, pp. 829–848. College Station, TX.

45. D'Hondt, S. & Lindinger, M. 1994 A stable isotopic record of the Maastrichtian ocean-climate system: South Atlantic DSDP site 528. *Palaeogeogr. Palaeoclimatol. Palaeoecol.* **112**, 363–378. (doi:10.1016/0031-0182(94)90081-7)

46. Westerhold, T., Röhl, U., Donner, B., McCarren, H. K. & Zachos, J. C. 2011 A complete high-resolution Paleocene benthic stable isotope record for the central Pacific (ODP Site 1209). *Paleoceanography* **26**, PA2216. (doi:10.1029/2010PA002092)

47. Li, L. & Keller, G. 1998 Abrupt deep-sea warming at the end of the Cretaceous. *Geology* **26**, 995 –998. (doi:10.1130/0091-7613(1998)026<0995:ADSWAT>2.3.CO;2)

48. Thibault, N. & Gardin, S. 2010 The calcareous nannofossil response to the end-Cretaceous warm event in the Tropical Pacific. *Palaeogeogr. Palaeoclimatol. Palaeoecol.* **291**, 239–252.

49. Thibault, N. & Gardin, S. 2007 The late Maastrichtian nannofossil record of climate change in the South Atlantic DSDP Hole 525A. *Mar. Micropaleontol.* **65**, 163–184. (doi:10.1016/j.marmicro.2007.07.004)

50. Ehrendorfer, T. W. 1993 Late Cretaceous (Maestrichtian) Calcareous Nannoplankton Biogeography with Emphasis on Events Immediately Preceding the Cretaceous/Paleocene Boundary.

51. O'Connell, S. B. 1990 Variations in Upper Cretaceous and Cenozoic Calcium Carbonate Percentages, Maud Rise, Weddell Sea, Antarctica. *Proc. Ocean Drill. Program Sci. Results* **113**, 971–984.

52. Norris, R. D. et al. 2014 U1403. In *Paleogene Newfoundland Sediment Drifts*, pp. 98 pp. College Station, TX: Integrated Ocean Drilling Program.

53. Frank, T. D. & Arthur, M. A. 1999 Tectonic forcings of Maastrichtian ocean-climate evolution. *Paleoceanography* **14**, 103–117. (doi:10.1029/1998PA900017)

54. Kucera, M., Malmgren, B. A. & Sturesson, U. 1997 Foraminiferal dissolution at shallow depths of the Walvis Ridge and Rio Grande Rise during the latest Cretaceous: Inferences for deep-water circulation in the South Atlantic. *Palaeogeogr. Palaeoclimatol. Palaeoecol.* **129**, 195–212. (doi:10.1016/S0031-0182(96)00133-2)

55. Gerstel, J., Thunell, R. C., Zachos, J. C. & Arthur, M. A. 1986 The Cretaceous/Tertiary Boundary Event in the North Pacific: Planktonic foraminiferal results from Deep Sea Drilling Project Site 577, Shatsky Rise. *Paleoceanography* **1**, 97–117. (doi:10.1029/PA001i002p00097)

56. Stone, R. 2014 Back from the dead. *Science* **346**, 1281–1283. (doi:10.1126/science.346.6215.1281)

57. Hönisch, B. et al. 2012 The Geological Record of Ocean Acidification. *Science* **335**, 1058–1063.

(doi:10.1126/science.1208277)

58. Peterson, L. C. & Prell, W. L. 1985 Carbonate dissolution in recent sediments of the eastern equatorial Indian Ocean: preservation patterns and carbonate loss above the lysocline. *Mar. Geol.* **64**, 259–290.

59. Jansen, H., Zeebe, R. E. & Wolf-Gladrow, D. A. 2002 Modeling the dissolution of settling CaCO3 in the ocean. *Glob. Biogeochem. Cycles* **16**, 11–1. (doi:10.1029/2000GB001279)

60. D'Hondt, S., Inagaki, F., Alvarez-Zarikian, C. A. & Expedition 329 Scientists 2011 South Pacific Gyre Subseafloor Life. *Proc. Integr. Ocean Drill. Program* **329**. (doi:http://dx.doi.org/10.2204/iodp.proc.329.2011)

61. Berger, W. H., Kroenke, L. W., Mayer, L. A., Backman, J., Janecek, T. R., Krissek, L., Leckie, M. & Lyle, M. 1992 The record of Ontong Java Plateau: Main results of ODP Leg 130. *Geol. Soc. Am. Bull.* **104**, 954–972. (doi:10.1130/0016-7606(1992)104<0954:TROOJP>2.3.CO;2)

62. Caldeira, K., Rampino, M. R., Volk, T. & Zachos, J. C. 1990 Biogeochemical modeling at mass extinction boundaries: Atmospheric carbon dioxide and ocean alkalinity at the K/T boundary. In *Extinction Events in Earth History* (eds E. G. Kauffman & O. H. Walliser), pp. 333–345. Berlin/Heidelberg: Springer-Verlag. [cited 2015 Jun. 17].

63. Caldeira, K. & Rampino, M. R. 1993 Aftermath of the end-Cretaceous mass extinction: Possible biogeochemical stabilization of the carbon cycle and climate. *Paleoceanography* **8**, 515–525. (doi:10.1029/93PA01163)

64. Bown, P. 2005 Selective calcareous nannoplankton survivorship at the Cretaceous-Tertiary boundary. *Geology* **33**, 653–656. (doi:10.1130/G21566AR.1)

65. Smit, J. 1982 Extinction and evolution of planktonic foraminifera after a major impact at the Cretaceous/Tertiary boundary. *Geol. Soc. Am. Spec. Pap.* **190**, 329–352. (doi:10.1130/SPE190-p329)

66. Cermeno, P., Dutkiewicz, S., Harris, R. P., Follows, M., Schofield, O. & Falkowski, P. G. 2008 The role of nutricline depth in regulating the ocean carbon cycle. *Proc. Natl. Acad. Sci.* **105**, 20344–20349. (doi:10.1073/pnas.0811302106)

67. Barclay, R. S. & Wing, S. L. 2016 Improving the Ginkgo CO2 barometer: Implications for the early Cenozoic atmosphere. *Earth Planet. Sci. Lett.* **in press**. (doi:10.1016/j.epsl.2016.01.012)

68. Minoletti, F., de Rafelis, M., Renard, M., Gardin, S. & Young, J. 2005 Changes in the pelagic fine fraction carbonate sedimentation during the Cretaceous–Paleocene transition: contribution of the separation technique to the study of Bidart section. *Palaeogeogr. Palaeoclimatol. Palaeoecol.* **216**, 119–137. (doi:10.1016/j.palaeo.2004.10.006)

69. Keller, G. & Abramovich, S. 2009 Lilliput effect in late Maastrichtian planktic foraminifera: Response to environmental stress. *Palaeogeogr. Palaeoclimatol. Palaeoecol.* **284**, 47–62. (doi:10.1016/j.palaeo.2009.08.029)

70. Keller, G. 2003 Biotic effects of impacts and volcanism. *Earth Planet. Sci. Lett.* **215**, 249–264.

71. Pospichal, J. J. 1994 Calcareous nannofossils at the K-T boundary, El Kef: No evidence for stepwise, gradual, or sequential extinctions. *Geology* **22**, 99. (doi:10.1130/0091-7613(1994)022<0099:CNATKT>2.3.CO;2)

72. Oliver, T. H. et al. 2015 Biodiversity and Resilience of Ecosystem Functions. *Trends Ecol. Evol.* **30**, 673–684. (doi:10.1016/j.tree.2015.08.009)

73. Paris, G., Donnadieu, Y., Beaumont, V., Fluteau, F. & Goddéris, Y. 2015 Geochemical consequences of intense pulse-like degassing during the onset of the Central Atlantic Magmatic Province. *Palaeogeogr. Palaeoclimatol. Palaeoecol.* (doi:10.1016/j.palaeo.2015.04.011)

74. Campbell, I. H., Czamanske, G. K., Fedorenko, V. A., Hill, R. I. & Stepanov, V. 1992 Synchronism of the Siberian Traps and the Permian-Triassic boundary. *Science* **258**, 1760–1763.

75. Birch, H., Coxall, H. K., Pearson, P. N., Kroon, D. & Schmidt, D. N. submitted Partial collapse of the marine biological pump at the Cretaceous-Paleogene boundary. *Geology*

76. Sepúlveda, J., Wendler, J. E., Summons, R. E. & Hinrichs, K.-U. 2009 Rapid Resurgence of Marine Productivity After the Cretaceous-Paleogene Mass Extinction. *Science* **326**, 129–132.

(doi:10.1126/science.1176233)

77. Coxall, H. K., D'Hondt, S. & Zachos, J. C. 2006 Pelagic evolution and environmental recovery after the Cretaceous-Paleogene mass extinction. *Geology* **34**, 297–300. (doi:10.1130/G21702.1)

78. Hull, P. M. 2015 Life in the aftermath of mass extinctions. *Curr. Biol.* **25**, R941–R952. (doi:10.1016/j.cub.2015.08.053)

79. Dutkiewicz, S., Morris, J. J., Follows, M. J., Scott, J., Levitan, O., Dyhrman, S. T. & Berman-Frank, I. 2015 Impact of ocean acidification on the structure of future phytoplankton communities. *Nat. Clim. Change* (doi:10.1038/nclimate2722)

80. Hull, P. M., Norris, R. D., Bralower, T. J. & Schueth, J. D. 2011 A role for chance in marine recovery from the end-Cretaceous extinction. *Nat. Geosci.* **4**, 856–860. (doi:10.1038/ngeo1302)

81. Zachos, J. C., Arthur, M. A., Thunell, R. C., Williams, D. F. & Tappa, E. J. 1985 Stable Isotope and Trace Element Geochemistry of Carbonate Sediments across the Cretaceous/Tertiary Boundary at Deep Sea Drilling Project Hole 577, Leg 86. *Initial Rep. Deep Sea Drill. Proj.* **86**, 513–532.

82. Birch, H. S., Coxall, H. K. & Pearson, P. N. 2012 Evolutionary ecology of Early Paleocene planktonic foraminifera: size, depth habitat and symbiosis. *Paleobiology* **38**, 374–390. (doi:10.1666/11027.1)

83. Schueth, J. D., Bralower, T. J., Jiang, S. & Patzkowsky, M. E. 2015 The role of regional survivor incumbency in the evolutionary recovery of calcareous nannoplankton from the Cretaceous/Paleogene (K/Pg) mass extinction. *Paleobiology* **41**, 661–679. (doi:10.1017/pab.2015.28)

Figure and table captions

Figure 1: Environmental changes coincident with Phase II Deccan Volcanism. Compilation of published Os isotope[39] (a), and $\delta^{18}O$-derived temperature[44–47] (b) records, alongside new (e,g) and published [39,50–52,54,55] (c,d,f,h) records of carbonate preservation in the lead up to the K-Pg boundary. Deccan emplacement is marked at the onset of Os isotope decline. In panel B, the dashed line is a 6^{th} order polynomial fit through the data, and the black solid line is a cubic spline. Note wt. % $CaCO_3$ Records from ODP Site 690 are subject to intense bioturbation near the K-Pg boundary; this region is marked as a dashed line. Os isotope decrease towards the boundary from 66.1 Ma is due to down-core leaching of extra-terrestrial Os [39]. Age constraints for DSDP 577 [55] (h) are uncertain below the onset of magnetochron C29r. All data are plotted against time (in million years ago, or Ma); for details of the age models used, see Supplementary Information.

Figure 2. Enhanced $CaCO_3$ preservation following the K-Pg boundary. Records of wt. % coarse Fraction (Panel a) from IODP Site 1209 [46], DSDP 577 [81], IODP U1403 [this study], IODP 1262 [80] and IODP 1267 [this study]. In the bottom panel (Panel b), records of fragmentation of planktonic foraminifera from DSDP Sites 528 and 577 [43] and IODP Site 1209 [28, this study]. Species richness bars above data panels are schematic representations of data from [82,83]. All data are plotted against time (in million years ago, or Ma); for details of the age models used, see Supplementary Information.

Figure 3. LOSCAR[31] simulations of Deccan degassing release and K-Pg reduction in $CaCO_3$ flux. Simulations of atmospheric pCO_2 (Panel A) and deep-water calcite saturation state (Panel B) response to simulated perturbations. Maximum and minimum CO_2 and SO_2 efflux estimates for Deccan eruptions are from ref. [16], partitioned into a main eruptive phase ('Phase II') beginning at the onset of C29r (86.5%) and a later one (13.5%) at the close of C29r in the Danian ('Phase III') [39]. $CaCO_3$ flux changes impact the $CaCO_3$:C_{org} ratio assuming no change in organic flux. Reduction in biological pump efficiency reduces the efficiency of the biological pump in utilising the parameterised nutrient pool (see Supplementary Discussion for more details). Model outputs are plotted against simulated model years, relative to the simulated K-Pg boundary.

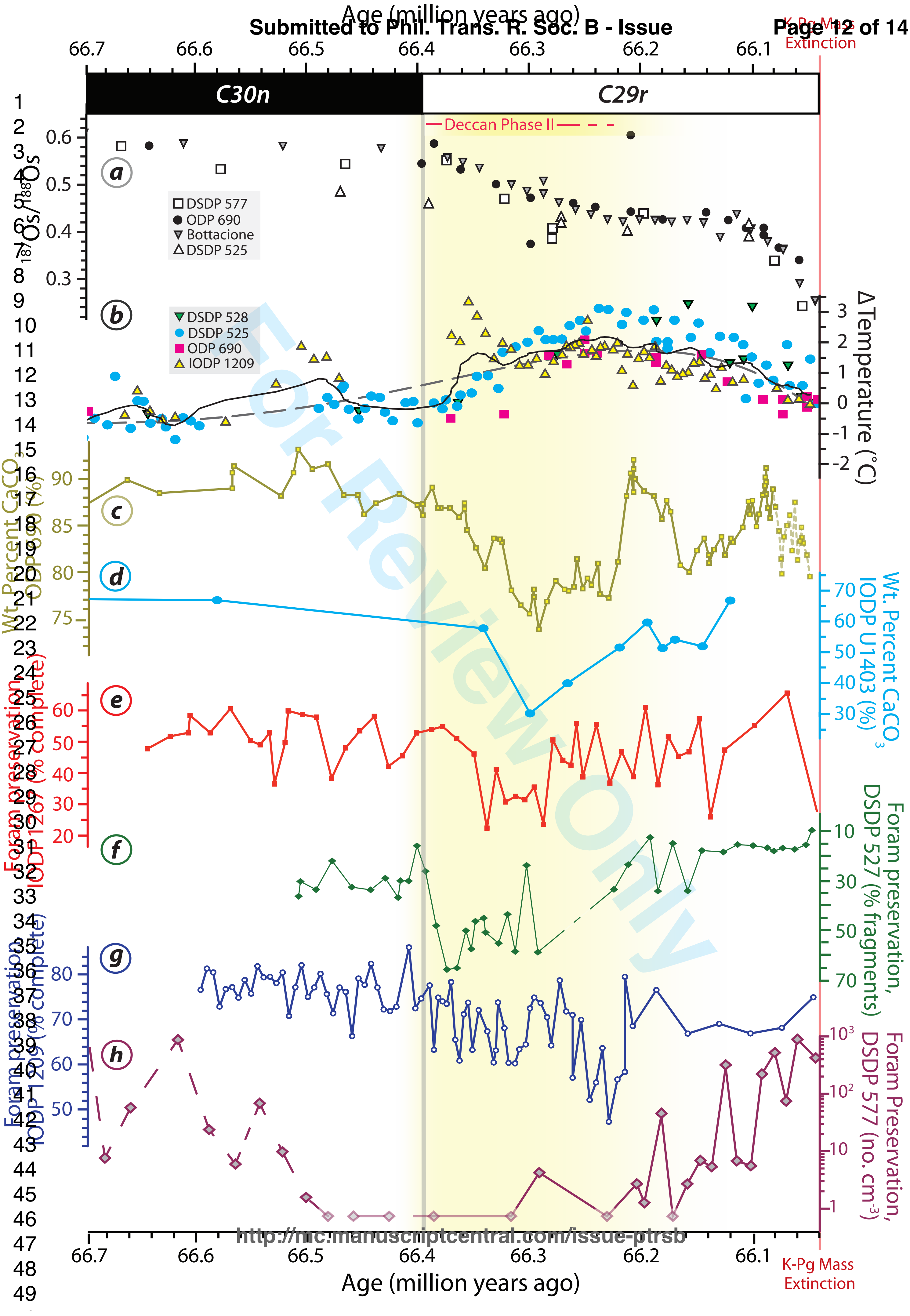
Age (million years ago)
66.7
66.6
66.5
66.4
66.3
66.2
66.1
K-Pg Mass Extinction
C30n
C29r
Deccan Phase II
a
$^{187}Os/^{188}Os$
0.6
0.5
0.4
0.3
DSDP 577
ODP 690
Bottacione
DSDP 525
b
DSDP 528
DSDP 525
ODP 690
IODP 1209
ΔTemperature (°C)
3
2
1
0
-1
-2
c
Wt. Percent $CaCO_3$ ODP 690 (%)
90
85
80
75
d
Wt. Percent $CaCO_3$ IODP U1403 (%)
70
60
50
40
30
e
Foram preservation IODP1267 (% complete)
60
50
40
30
20
f
Foram preservation, DSDP 527 (% fragments)
10
30
50
70
g
Foram preservation IODP 1209 (% complete)
80
70
60
50
h
Foram Preservation, DSDP 577 (no. cm^{-3})
10^3
10^2
10
1
Age (million years ago)

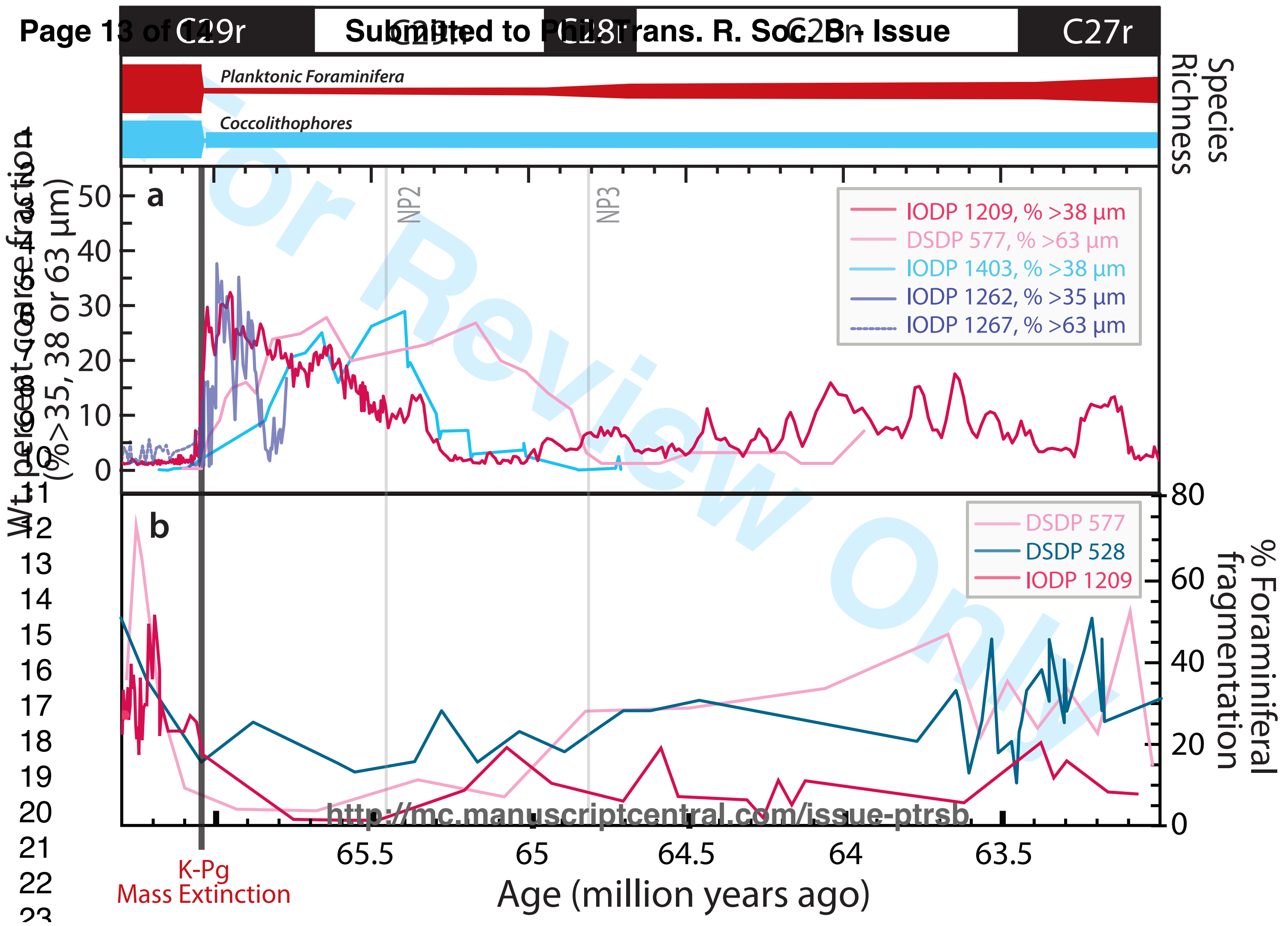
C29r
C29n
C28r
C28n
C27r
Species Richness
Planktonic Foraminifera
Coccolithophores
a
NP2
NP3
IODP 1209, % >38 µm
DSDP 577, % >63 µm
IODP 1403, % >38 µm
IODP 1262, % >35 µm
IODP 1267, % >63 µm
Wt. percent coarse fraction (%>35, 38 or 63 µm)
b
DSDP 577
DSDP 528
IODP 1209
% Foraminiferal fragmentation
K-Pg Mass Extinction
Age (million years ago)
65.5
65
64.5
64
63.5

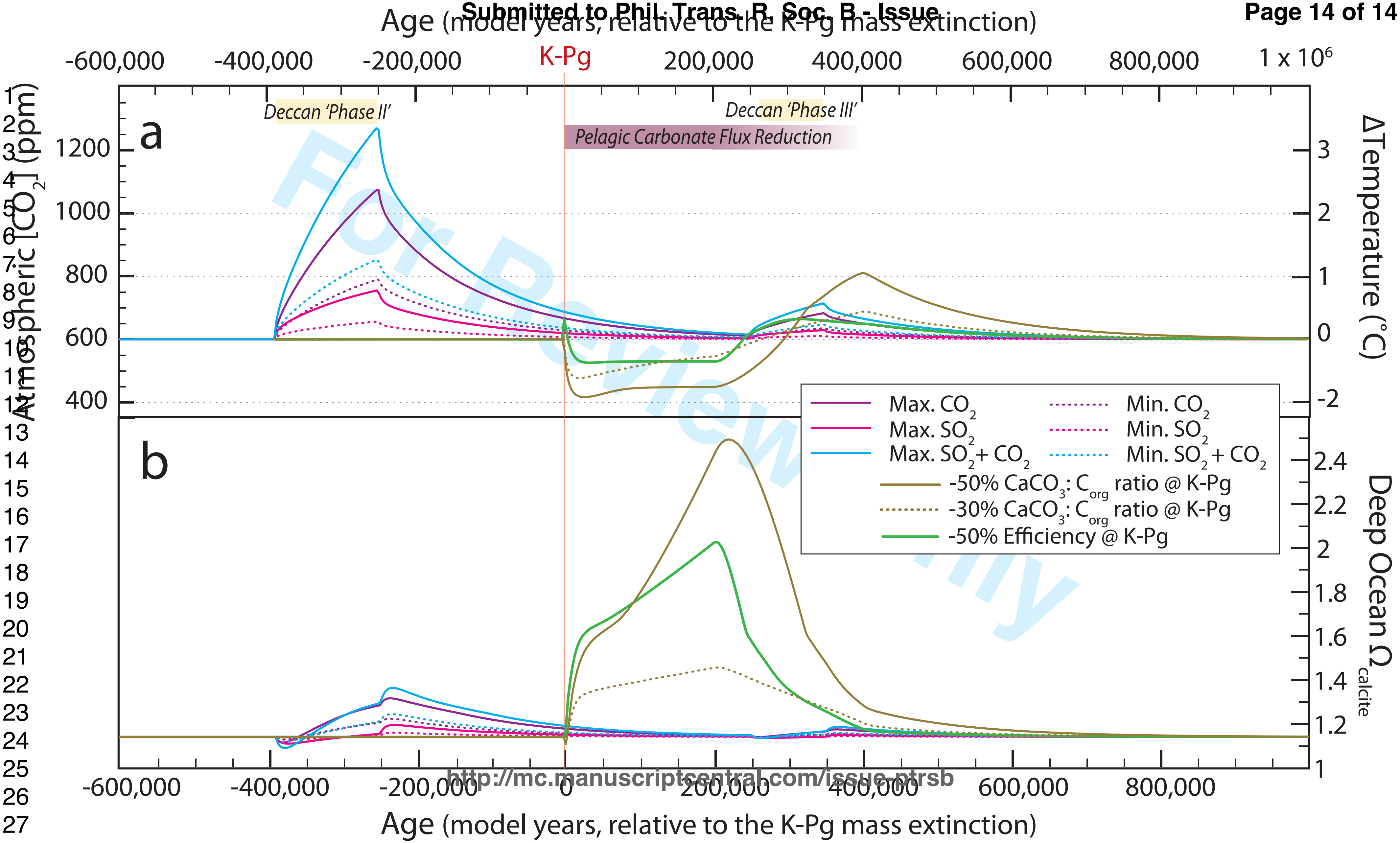
Age (model years, relative to the K-Pg mass extinction)
-600,000
-400,000
-200,000
K-Pg
200,000
400,000
600,000
800,000
1 x 10^6
a
Deccan 'Phase II'
Deccan 'Phase III'
Pelagic Carbonate Flux Reduction
Atmospheric [CO2] (ppm)
1200
1000
800
600
400
ΔTemperature (°C)
3
2
1
0
-2
b
Max. CO2
Max. SO2
Max. SO2 + CO2
Min. CO2
Min. SO2
Min. SO2 + CO2
-50% CaCO3: Corg ratio @ K-Pg
-30% CaCO3: Corg ratio @ K-Pg
-50% Efficiency @ K-Pg
Deep Ocean Ω calcite
2.4
2.2
2
1.8
1.6
1.4
1.2
1
-600,000
-400,000
-200,000
0
200,000
400,000
600,000
800,000
Age (model years, relative to the K-Pg mass extinction)